Discrete update pose filter on the special Euclidean group SE(3)

M. Zamani[1] and J. Trumpf[2]

***Abstract*— This paper proposes two variants of the Geometric Approximate Minimum Energy (GAME) filter on the Special Euclidean Group SE(3) in the case that exteroceptive measurements are obtained in discrete time. Continuous-discrete versions of the GAME filter are provided that near-continuously predict pose and its covariance using high frequency interoceptive measurements and then update these estimates utilizing low frequency exteroceptive measurements obtained in discrete time. The two variants of the proposed filter are differentiated in their derivation due to the choice of affine connection used on SE(3). The proposed discrete update filters are derived based on first principles of deterministic minimum-energy filtering extended for discrete time measurements and derived directly on SE(3). The performance of the proposed filters is demonstrated and compared in simulations with a short discussion of practical implications of the choice of affine connection.**

I. INTRODUCTION

This paper is concerned with filters used for estimating the position and attitude (together referred to as pose) of a moving rigid-body using noisy interoceptive velocity and exteroceptive vector measurements that bear information on the pose. Pose estimation has many applications in autonomous systems and is a fundamental building block of many control, vision and robotic problems. The literature for pose estimation methods goes back to the early applications in space explorations (see [1], [2] and references therein).

The Extended Kalman Filter (EKF) [3], which is based on applying the optimal Kalman filter [4] to the linearized equations of nonlinear problems, is perhaps the best known generic engineering tool for performing state estimation on systems with nonlinear dynamics. While the EKF has traditionally been applied to the pose filtering problem as well, more recent methods take advantage of the symmetries inherent in the nonlinear space of attitude and pose models in order to improve the estimation performance.

Early accounts of nonlinear attitude and pose estimation methods can be found in [1], [2], [5], [6] and the references therein. In this work, we focus on nonlinear pose filters with time-varying gains, as opposed to nonlinear constant gain observers for attitude and pose estimation [6]–[13]. A number of geometric nonlinear filtering approaches applicable to attitude and pose estimation problems exist in the literature. Among those, the Multiplicative Extended Kalman Filter (MEKF) [1] and the variants of the Invariant EKF (IEKF) [14]–[16] utilize a nonlinear Lie group structure of the observer state space which includes a linear space innovation term. The dynamics of the innovation term is then derived based on Kalman filtering resulting in a time-varying gain equation where the overall filter preserves the Lie group (symmetric) structures of the attitude and pose spaces. These works have shown improved performance over non-geometric implementations of the EKF for attitude and pose filtering. Our earlier works [17], [18] similarly preserve the Lie group (symmetric) structures of the attitude and pose spaces but are derived based on adapting the first principles of least squares deterministic filtering design [19], [20] to the nonlinear Lie group kinematic equations of attitude and pose. As a result, we proposed additional terms in the resulting Riccati equation that bear information on second order derivatives of the filtering cost function, not previously taken advantage of in the attitude and pose filtering literature. On the other hand, [14], [21] and some similar methods have additionally offered convergence and stability results for their proposed filters. These questions are outside the scope of this work. The papers [6], [8] include a stability analysis of the observer error system. The aforementioned methods have been benchmarked against a nonlinear complimentary observer [6] in [22] where their performances were observed to be comparable.

In this work, we extend our previously proposed continuous-time Geometric Approximate Minimum Energy (GAME) filter on the Special Euclidean Group SE(3) [18] to a continuous-discrete formulation. The derivation is based on first principles least squares filtering and the variational analysis adapted to the Lie group structure of the special Euclidean group $\mathrm{SE}(3)$. We prove that the continuous propagation of the left-invariant kinematics based on velocity measurements is the optimal solution to the continuous-time least squares minimum-energy filtering problem. Moreover, using a quadratic assumption on the value function of the problem we derive the discrete update step on $\mathrm{SE}(3)$ as the optimal solution of the point optimization problem concerning fusion between the discrete measurement error energy and the continuous-time value function. Two versions of the continuous-discrete filter are derived based on the choice of affine connection on $\mathrm{SE}(3)$. We provide a simulation study that demonstrates the performance of the proposed filters in a scenario with large measurement errors and low frequency discrete landmark measurements.

The remainder of the paper is structured as follows. Section II contains some preliminary notions required later on for the geometric formulation of the filtering problem. An extensive account of useful definitions of operators, errors, metrics and projections on the Lie group spaces of $\mathrm{SO}(3)$

[1]is with the Land Division, DST, Australia, email : mohammad.zamani@dst.defence.gov.au, [2]is with the Research School of Electrical, Energy and Materials Engineering, Australian National University, Canberra, ACT, 2601 Australia, and the Australian Centre for Robotic Vision (ACRV) http://www.roboticvision.org. email:jochen.trumpf@anu.edu.au

and $\mathrm{SE}(3)$ along with some identities are provided that facilitate the arguments of the subsequent sections. Section III formally introduces our continuous and discrete pose filtering problems as deterministic least squares optimization problems. Section IV contains our main results including the proposed filters, their underlying assumptions and the proofs of their optimality. We illustrate the performance of the proposed filters in Section V and finally Section VI concludes the paper.

II. PRELIMINARIES

Let $\mathcal{A}$ denote the global reference frame and $\mathcal{B}$ denote a body fixed frame to a moving rigid body in 3D space. Translation of $\mathcal{B}$ with respect to $\mathcal{A}$, expressed in $\mathcal{A}$, is denoted as $p \in \mathbb{R}^3$. The attitude (orientation) of $\mathcal{B}$ relative to the reference frame $\mathcal{A}$ is represented by a rotation matrix $R \in \mathrm{SO}(3)$. The rotation group is denoted by $\mathrm{SO}(3) = \{R \in \mathbb{R}^{3\times 3} \,|\, R^\top R = I, \det(R) = 1\}$, where $(.)^\top$ is the transpose map, I is the 3 by 3 identity matrix and $\det(.)$ is the matrix determinant. The associated Lie algebra $\mathfrak{so}(3)$ is the set of skew-symmetric matrices, $\mathfrak{so}(3) = \{\omega_\times \in \mathbb{R}^{3\times 3} \,|\, \omega_\times = -\omega_\times^\top\}$. For $\omega = [\omega_1, \omega_2, \omega_3]^\top \in \mathbb{R}^3$, the lower index operator $(.)_\times : \mathbb{R}^3 \longrightarrow \mathfrak{so}(3)$ yields the skew-symmetric matrix

$$\omega_\times \coloneqq \begin{bmatrix} 0 & -\omega_3 & \omega_2 \\ \omega_3 & 0 & -\omega_1 \\ -\omega_2 & \omega_1 & 0 \end{bmatrix}.$$

The skew-symmetric matrix is associated with the cross product by ω, *i.e.*, $\omega_\times v = \omega \times v$, for all $v \in \mathbb{R}^3$. Inversely, the operator $\mathbf{vex} : \mathfrak{so}(3) \longrightarrow \mathbb{R}^3$ extracts the skew coordinates, $\mathbf{vex}(\omega_\times) \coloneqq \omega$.

A pose matrix consisting of attitude R and translation p of the body fixed frame $\mathcal{B}$ with respect to the global reference frame $\mathcal{A}$ can be represented as $X = \begin{bmatrix} R & p \\ 0_{1\times 3} & 1 \end{bmatrix} \in \mathrm{SE}(3)$ where the special Euclidean group $\mathrm{SE}(3)$ is defined in the following.

$$\mathrm{SE}(3) = \{X = \begin{bmatrix} R & p \\ 0_{1\times 3} & 1 \end{bmatrix} \in \mathbb{R}^{4\times 4} \;\mid\; R \in \mathrm{SO}(3),\; p \in \mathbb{R}^3\}. \tag{1}$$

This representation, commonly known as homogeneous coordinates, preserves the group structure of $\mathrm{SE}(3)$ with matrix multiplication, *i.e.*, $X_1 X_2 \in \mathrm{SE}(3)$ for all $X_1, X_2 \in \mathrm{SE}(3)$. The associated inverse pose X^{-1}, which is also an element of $\mathrm{SE}(3)$, is given by

$$X^{-1} = \begin{bmatrix} R^\top & -R^\top p \\ 0_{1\times 3} & 1 \end{bmatrix}.$$

The associated Lie algebra is the set of twist matrices in $\mathfrak{se}(3)$.

$$\mathfrak{se}(3) = \left\{\Gamma \coloneqq \begin{bmatrix} (\Gamma_\omega)_\times & \Gamma_v \\ 0_{1\times 3} & 0 \end{bmatrix} \in \mathbb{R}^{4\times 4} \mid \Gamma_\omega, \Gamma_v \in \mathbb{R}^3 \right\}. \tag{2}$$

The map $(.)^\wedge : \mathbb{R}^6 \longrightarrow \mathfrak{se}(3)$ and its inverse $(.)^\vee : \mathfrak{se}(3) \longrightarrow \mathbb{R}^6$ are defined as

$$\begin{bmatrix} \Gamma_\omega \\ \Gamma_v \end{bmatrix}^\wedge \coloneqq \begin{bmatrix} (\Gamma_\omega)_\times & \Gamma_v \\ 0_{1\times 3} & 0 \end{bmatrix},\; (\begin{bmatrix} \Gamma_\omega \\ \Gamma_v \end{bmatrix}^\wedge)^\vee \coloneqq \begin{bmatrix} \Gamma_\omega \\ \Gamma_v \end{bmatrix}. \tag{3}$$

Let $T_X \mathrm{SE}(3)$ denote the linear space tangent to the manifold of $\mathrm{SE}(3)$ at X. Note that the Lie algebra $\mathfrak{se}(3)$ coincides with $T_I \mathrm{SE}(3)$. For all $\Gamma \in \mathfrak{se}(3)$, the tangent vector $X\Gamma \in T_X \mathrm{SE}(3)$. Consider the following definitions.

$$\frac{\mathbf{1}}{\mathbf{2}} \coloneqq \begin{bmatrix} \frac{1}{2} I_{3\times 3} & 0_{3\times 1} \\ 0_{1\times 3} & 1 \end{bmatrix},\; \mathbf{2} \coloneqq \begin{bmatrix} 2 I_{3\times 3} & 0_{3\times 1} \\ 0_{1\times 3} & 1 \end{bmatrix},$$

and let the metric $\langle .,. \rangle_X : T_X \mathrm{SE}(3) \times T_X \mathrm{SE}(3) \longrightarrow \mathbb{R}$ denote the standard left-invariant Riemannian metric on $\mathrm{SE}(3)$. For $\Gamma, \Omega \in \mathfrak{se}(3)$ the following definitions hold.

$$\begin{aligned} \langle X\Gamma, X\Omega \rangle_X &= \langle \Gamma, \Omega \rangle_I \coloneqq \langle \Gamma, \Omega \rangle \\ &\coloneqq \mathbf{trace}(\frac{\mathbf{1}}{\mathbf{2}} \Gamma^\top \Omega) \coloneqq \langle \Gamma^\vee, \Omega^\vee \rangle \coloneqq (\Gamma^\vee)^\top \Omega^\vee. \end{aligned} \tag{4}$$

Here, $\mathbf{trace}(.) : \mathbb{R}^{n\times n} \longrightarrow \mathbb{R}$ is the matrix trace function. Let $\mathbb{P} : \mathbb{R}^{4\times 4} \to \mathfrak{se}(3)$ denote the unique orthogonal projection of $\mathbb{R}^{4\times 4}$ onto $\mathfrak{se}(3)$ with respect to the inner product $\langle \cdot, \cdot \rangle$, *i.e.*, for all $\Gamma \in \mathfrak{se}(3)$, $M \in \mathbb{R}^{4\times 4}$, one has

$$\langle \Gamma, M \rangle = \langle \Gamma, \mathbb{P}(M) \rangle = \langle \mathbb{P}(M), \Gamma \rangle.$$

One verifies that for all $M_1 \in \mathbb{R}^{3\times 3}, m_{2,3} \in \mathbb{R}^3, m_4 \in \mathbb{R}$,

$$\mathbb{P}\left(\begin{bmatrix} M_1 & m_2 \\ m_3^\top & m_4 \end{bmatrix}\right) = \begin{bmatrix} \mathbb{P}_a(M_1) & m_2 \\ 0_{1\times 3} & 0 \end{bmatrix}.$$

Given any matrix $M \in \mathbb{R}^{n\times n}$, its symmetric and skew-symmetric projections are defined as $\mathbb{P}_s(M) \coloneqq 1/2(M + M^\top)$ and $\mathbb{P}_a(M) \coloneqq 1/2(M - M^\top)$, respectively.

For any two $\mathrm{SE}(3)$ elements X_1, X_2 and a positive definite matrix $P \in \mathbb{R}^{6\times 6} > 0$, their weighted Euclidean distance is defined next.

$$\|X_1 - X_2\|_P \coloneqq \sqrt{\langle (P\,\mathbf{log}(X_2^{-1} X_1)^\vee)^\wedge, \mathbf{log}(X_2^{-1} X_1) \rangle}. \tag{5}$$

Note that $\mathbf{log}(.) : \mathfrak{se}(3) \longrightarrow \mathrm{SE}(3)$ is the matrix logarithm on $\mathrm{SE}(3)$.

A. Differential Geometric Notions

Let $f : \mathrm{SE}(3) \longrightarrow \mathbb{R}$ denote a differentiable map. Then $\mathcal{D}_X f(X) : T_X \mathrm{SE}(3) \longrightarrow \mathbb{R}$ denotes the differential map defined below.

$$\mathcal{D}_X f(X) \circ (X\Gamma) = \langle \nabla_X f(X), X\Gamma \rangle_X. \tag{6}$$

Here, $\Gamma \in \mathfrak{se}(3)$, $X\Gamma \in T_X \mathrm{SE}(3)$ is a tangent direction towards which the differential is calculated. The left invariant metric $\langle .,. \rangle$ was introduced in (4) and $\nabla_X f(X) \in T_X \mathrm{SE}(3)$ is the gradient. Similarly, the second order differential map $\mathcal{D}_X^2 f(X) : T_X \mathrm{SE}(3) \times T_X \mathrm{SE}(3) \longrightarrow \mathbb{R}$ is defined next.

$$\begin{aligned} &\mathcal{D}_X^2 f(X) \circ (X\Gamma, X\Xi) = \langle \mathbf{Hess}_X\, f(X) \circ X\Psi, X\Gamma \rangle_X \\ &= \langle \mathbf{Hess}_X\, f(X) \circ X\Gamma, X\Psi \rangle_X. \end{aligned} \tag{7}$$

Here, $\Gamma, \Psi \in \mathfrak{se}(3)$ and the Hessian $\mathbf{Hess}_X\, f(X) : T_X \mathrm{SE}(3) \longrightarrow T_X \mathrm{SE}(3)$ is a symmetric mapping with respect to the left invariant metric. In another form,

$$\begin{aligned} &\mathcal{D}_X^2 f(X) \circ (X\Gamma, X\Psi) = \\ &D_X(\mathcal{D}_X f(X) \circ (X\Gamma)) \circ X\Psi - \langle \nabla_X f(X), X\, \mathbf{\Lambda}_\Psi(\Gamma) \rangle_X. \end{aligned}$$

Here, $\mathbf{\Lambda}_\Psi(.) : \mathfrak{se}(3) \longrightarrow \mathfrak{se}(3)$ is the connection function. In this paper we will utilize the following two connection functions on $\mathrm{SE}(3)$. Consider two elements of the Lie algebra $\Gamma, \Psi \in \mathfrak{se}(3)$. The first connection utilized is the $0-$connection.

$$\mathbf{\Lambda}^0_\Psi(\Gamma) \coloneqq \mathbb{P}(\Psi\Gamma). \tag{8}$$

The second connection utilized in this paper is the symmetric Cartan connection.

$$\mathbf{\Lambda}^C_\Psi(\Gamma) \coloneqq \frac{1}{2}[\Psi, \Gamma] \coloneqq \frac{1}{2}(\Psi\Gamma - \Gamma\Psi). \tag{9}$$

Here, $[.,.] : \mathfrak{se}(3) \times \mathfrak{se}(3) \longrightarrow \mathfrak{se}(3)$ is the Lie bracket of $\mathfrak{se}(3)$. One verifies that the following identities holds.

$$\begin{aligned}(\mathbf{\Lambda}^0_\Psi(\Gamma))^\vee &= \begin{bmatrix} \frac{1}{2}\Psi_\omega \times \Gamma_\omega \\ \Psi_\omega \times \Gamma_v \end{bmatrix}, \\ (\mathbf{\Lambda}^C_\Psi(\Gamma))^\vee &= \frac{1}{2}\begin{bmatrix} \Psi_\omega \times \Gamma_\omega \\ \Psi_\omega \times \Gamma_v - \Gamma_\omega \times \Psi_v \end{bmatrix}. \end{aligned} \tag{10}$$

Note that for every $\Omega_\times \in \mathfrak{so}(3)$, $M \in \mathbb{R}^{3\times 3}$ and $S = S^\top \in \mathbb{R}^{3\times 3}$,

$$\mathbf{trace}(\Omega_\times \mathbb{P}_s(M)) = 0,\ \mathbf{trace}(\mathbb{P}_s(S\Omega_\times)) = 0. \tag{11}$$

Let $\mathbb{S}^{n\times n}$ denote the set of symmetric matrices, and $\mathbb{P}_t(.) : \mathbb{S}^{n\times n} \longrightarrow \mathbb{S}^{n\times n}$ denote the mapping defined in the following for $S \in \mathbb{S}^{3\times 3}$.

$$\mathbb{P}_t(S) \coloneqq \mathbf{trace}(S)I - S. \tag{12}$$

The following identities hold for every $\gamma, \psi \in \mathbb{R}^3$, $R \in \mathrm{SO}(3)$.

$$\gamma_\times \psi_\times = \psi\gamma^\top - \gamma^\top \psi I. \tag{13}$$

$$\psi \times \gamma = \psi_\times \gamma = 2\,\mathbf{vex}\,\mathbb{P}_a(\gamma\psi^\top) = 2\,\mathbf{vex}\,\mathbb{P}_a(\psi_\times\gamma_\times). \tag{14}$$

$$\mathbb{P}_a(S\gamma_\times) = \frac{1}{2}(\mathbb{P}_t(S)\gamma)_\times. \tag{15}$$

$$\mathbf{trace}(\gamma_\times^\top S\psi_\times) = \gamma^\top \mathbb{P}_t(S)\psi. \tag{16}$$

III. Problem Formulation

In this section we state the left invariant kinematics on $\mathrm{SE}(3)$, introduce models for interoceptive and exteroceptive measurements and formalize the filtering problem using these models.

A. Pose Kinematics

Let $X = \begin{bmatrix} R & p \\ 0_{1\times 3} & 1 \end{bmatrix}$ denote the pose matrix of a moving body in 3D space. The left invariant pose kinematics on $\mathrm{SE}(3)$ is given by

$$\dot{X} = X \begin{bmatrix} \Omega \\ V \end{bmatrix}^\wedge,\ X(0) = X_0. \tag{17}$$

Recall that $R \in \mathrm{SO}(3)$ is the attitude and $p \in \mathbb{R}^3$ the translation of the body fixed frame $\mathcal{B}$ with respect to the global reference frame $\mathcal{A}$. The matrix $\begin{bmatrix} \Omega \\ V \end{bmatrix}^\wedge \in \mathfrak{se}(3)$ is the twist and embodies the angular velocity $\Omega \in \mathbb{R}^3$ and translational velocity $V \in \mathbb{R}^3$ of the body fixed frame $\mathcal{B}$ with respect to the global reference frame $\mathcal{A}$.

B. Interoceptive Velocity Measurements

The measured twist is comprised of angular and translational velocity measured in the body fixed frame $\mathcal{B}$ as represented by the following equations

$$\begin{aligned} &U \coloneqq \begin{bmatrix} \Omega \\ V \end{bmatrix}^\wedge + (B\delta)^\wedge,\ B \coloneqq \begin{bmatrix} B_\omega & 0_{3\times 3} \\ 0_{3\times 3} & B_v \end{bmatrix},\ \delta \coloneqq \begin{bmatrix} \delta_\omega \\ \delta_v \end{bmatrix}, \\ &U_\omega = \Omega + B_\omega\delta_\omega,\ U_v = V + B_v\delta_v, \end{aligned} \tag{18}$$

where $B_\omega, B_v \in \mathbb{R}^{3\times 3}$ are measurement error coefficient matrices determined from the sensor properties while $\delta_\omega, \delta_v \in \mathbb{R}^3$ are the unknown (here assumed zero mean) angular and translational velocity errors incurred in the measurement process.

C. Exteroceptive Landmark Measurements

One can indirectly obtain further information on the pose of a moving body by measuring the position of a known landmark in the body fixed frame and by comparing the measurement against the a priori known position of that landmark in the global reference frame.

$$\bar{y} = X^{-1}\bar{l} + \tilde{D}\mathring{\epsilon},\ \tilde{D} \coloneqq \begin{bmatrix} D & 0_{3\times 1} \\ 0_{1\times 3} & 1 \end{bmatrix}. \tag{19}$$

Here the mappings $\bar{(.)}, \mathring{(.)} : \mathbb{R}^3 \longrightarrow \mathbb{R}^4$ are defines as $\bar{x} \coloneqq [x, 1]^\top$ and $\mathring{x} \coloneqq [x, 0]^\top$, respectively. The vector $y \in \mathbb{R}^3$ is the measured landmark coordinates in $\mathcal{B}$, $l \in \mathbb{R}^3$ is the known true coordinates of the landmark in the global reference frame $\mathcal{A}$, $\epsilon \in \mathbb{R}^3$ is the measurement error incurred in $\mathcal{B}$ and where $D \in \mathbb{R}^{3\times 3}$ is the measurement error coefficient matrix determined based on the sensor properties.

Equation (19) is alternatively expressed as

$$y = R^\top(l - p) + D\epsilon. \tag{20}$$

Note that well-posedness of the full six degree of freedom pose filtering problem typically relies on at least three non-collinear fixed landmark measurements of the type introduced in (20) [23].

D. The Filtering Problem

The interoceptive velocity measurements (18) are often available with a high update rate (relative to exteroceptive measurements) and can approximately be accounted for as continuous signals. Following the deterministic minimum-energy filtering formalism, that was first introduced by Mortensen [19] and later refined in [20], let us consider the continuous-time filtering cost

$$J_t(X, \delta) \coloneqq \frac{1}{2}\|X(0) - \hat{X}_0\|^2_{P_0} + \frac{1}{2}\int_0^t \|\delta\|^2 d\tau. \tag{21}$$

The first term in (21) is the squared Euclidean distance initialization error between the true pose $X(0)$ and a priori known estimate of it $\hat{X}_0 \in \mathrm{SE}(3)$ defined according to (5) with the positive definite weight matrix $P_0 \in \mathbb{R}^{6\times 6}$. The second integral term in (21) is the accumulated squared Euclidean norm of the velocity measurement error discussed in (18).

Problem 1 (Dead-Reckoning): Given the velocity measurement data sequence $U^\vee|_{[0,t]}$ obtained according to the model (18) in the period $[0,t]$ find the pose estimate $\hat{X}(t) \in \mathrm{SE}(3)$ for the current true pose state $X(t)$ of system (17) such that the cost $J_t(X,\delta)$ defined in (21) is minimized. In other words, given the data $U^\vee|_{[0,t]}$, the a priori known entities B, $\hat{X}_0$ and P_0 and the models (17), (18) and (21) find the current minimum-energy estimate $\hat{X}(t)$ defined as the end point of the minimizing pose trajectory $X_t^*|_{[0,t]}$, i.e. $\hat{X}(t) \coloneqq X_t^*(t)$. Moreover, the estimate $\hat{X}(t)$ is to be calculated recursively, that is, $\hat{X}(t)$ is to be calculated based on the current time solution $\hat{X}(t)$ and the current velocity measurement $U^\vee(t)$.

Minimizing the cost (21) can in fact be broken into two steps. The first step is to minimize (21) over the measurement error trajectory $\delta|_{[0,t]}$ and the second step is to minimize (21) over the pose trajectory $X|_{[0,t]}$. The latter step can equivalently be simplified to minimizing (21) over a single point of the pose trajectory, e.g. the start point $X(0)$, the end point $X(t)$ or any other point in between. This is because, the first minimization step already yields a minimizing error trajectory $\delta^*|_{[0,t]}$ and that trajectory together with measurement data $U^\vee|_{[0,t]}$ and any single point of the pose trajectory $X|_{[0,t]}$ will yield the full minimizing pose trajectory $X^*|_{[0,t]}$.

The value of the first step minimization explained above, can be encoded using a value function defined next.

$$V(X,t) \coloneqq \min_{\delta|[0,t]} J_t(X,\delta),\ V(X(0),0) = \frac{1}{2}\|X(0)-\hat{X}_0\|^2_{P_0}. \tag{22}$$

The value function (22) provides an alternative definition for the minimum-energy estimate solution of Problem 1, i.e.

$$\hat{X}(t) \coloneqq \arg\min_X V(X,t)(t), \tag{23}$$

where X is any point of the true pose trajectory $X|_{[0,t]}$.

Interpreted differently, the value function (22) is an error energy or uncertainty measure for the true pose trajectory $X|_{[0,t]}$ at the time instance t. Accordingly, the estimate $\hat{X}(t)$ emerges as the minimizing point of this error energy measure and hence is called the minimum-energy estimate [19].

So far, Problem 1 is not concerned with the possibility of improving the estimated pose $\hat{X}(t)$ based on the exteroceptive measurements of the type introduced in (19). The following problem, assumes that a landmark measurement $\bar{y}(t)$ sporadically becomes available at time t and asks how to update the current estimate $\hat{X}(t)$ to a new estimate $\hat{X}^+(t)$ based on this new information. Upon close inspection, the unknown signal $\check{e}(t)$ can in fact be equally expressed in terms of the data $\bar{y}(t)$ and the unknown true pose $X(t)$. Therefore, we can introduce the following updated error energy measure for the true pose trajectory.

$$V^+(X,t) \coloneqq V(X,t) + \frac{1}{2}\|\bar{y}(t) - X^{-1}(t)\bar{l}\|^2_{(\bar{D}\bar{D}^\top)^{-1}}. \tag{24}$$

Problem 2 (Discrete Update): Given a current estimate $\hat{X}(t)$ of the true pose $X(t)$, i.e. a dead-reckoning solution of Problem 1, and a landmark measurement $\bar{y}(t)$ of the known landmark coordinates $\bar{l}$, obtained according to (19), find the minimum-energy estimate $\hat{X}^+(t)$ that minimizes the error energy cost (24). In other words, the task is to find

$$\hat{X}^+(t) \coloneqq \arg\min_X V^+(X,t)(t). \tag{25}$$

IV. Main Results

In this section we address the problems introduced in Section III and provide two distinct solutions based on the two choices of connections that were introduced in equations (8) and (9). Following our original work in [17], note the following assumptions and definition regarding the derivatives of the value function. We will utilize them throughout our subsequent results.

Assumption 1: The gradient and the Hessian with respect to X of the value function $V(X,t)$ (22) exist at the minimum point $X = \hat{X}(t)$. In other words, the value function is twice differentiable when evaluated at $X = \hat{X}(t)$.

Assumption 2: The value function $V(X,t)$ (22) is quadratic in X when evaluated at the minimum point $X = \hat{X}(t)$. In other words, the higher order derivatives of $V(X,t)$ vanish at $X = \hat{X}(t)$.

Note that the initial condition of the value function given in (22) is in agreement with these assumptions but in general no theoretical proof for these assumptions exist in the literature, that we are aware of.

Definition 1: Given any two tangent directions $X\Gamma, X\Psi \in T_X\,\mathrm{SE}(3)$, the Hessian $\mathbf{Hess}_X\, V(X,t)|_{X=\hat{X}(t)}$ acting as a symmetric mapping with respect to the inner product

$$\langle \mathbf{Hess}_X\, V(X,t) \circ X\Psi, X\Gamma\rangle_{X=\hat{X}(t)}$$

, as defined in (7), is equivalently represented with a positive definite matrix $P \in \mathbb{R}^{6\times 6}$ operating on vectors $\Gamma^\vee, \Psi^\vee \in \mathbb{R}^6$.

$$\langle P\Psi^\vee, \Gamma^\vee\rangle \coloneqq \langle \mathbf{Hess}_X\, V(X,t) \circ X\Psi, X\Gamma\rangle_{X=\hat{X}(t)}. \tag{26}$$

Following the classical optimal control/filtering literature and adapting the theory to our Lie group setup [17], let us define the Hamiltonian function associated with (21).

$$\mathcal{H}(X, X\mu^\wedge, \delta, t) \coloneqq \frac{1}{2}\|\delta\|^2 - \langle X\mu^\wedge, X(U-(B\delta)^\wedge)\rangle_X. \tag{27}$$

Here $X\mu^\wedge \in T_X\,\mathrm{SE}(3)$ is the co-state variable with $\mu^\wedge \in \mathfrak{se}(3)$.

Lemma 1: The optimal Hamiltonian (27) when minimized over $\delta(t)$ is given from

$$\begin{aligned}\mathcal{H}^*(X, X\mu^\wedge, t) &\coloneqq \min_{\delta(t)} \mathcal{H}(X, X\mu^\wedge, \delta, t)\\ &= -\frac{1}{2}\|\mu\|^2_{BB^\top} - \langle X\mu^\wedge, XU\rangle_X.\end{aligned} \tag{28}$$

The proof follows from the algebraic notions introduced in Section II and by checking that the minimizing argument is obtained as $\delta^*(t) = -B^\top\mu$.

Again, following the classical optimal control/filtering literature adapted to Lie groups [17] we obtain the Hamilton-Jacobi-Bellman (HJB) equation

$$\frac{\partial}{\partial t}V(X,t) = \mathcal{H}^*(X, \nabla_X V(X,t), t). \tag{29}$$

Here, $\frac{\partial}{\partial t}V(X,t)$ denotes the partial derivative of $V(X,t)$ with respect to its second argument t. It should be noted that the co-state $X\mu^\wedge$ is replaced in the optimal Hamiltonian with $\nabla_X V(X,t)$ which denotes the gradient of the value function with respect to X according to definition (6). Using $X\mu^\wedge = \nabla_X V(X,t)$ and the definitions given in (4), the minimum Hamiltonian (28) yields

$$\begin{aligned}\mathcal{H}^*(X,\nabla_X V(X,t),t) &= -\langle \nabla_X V(X,t), XU\rangle_X \\ &- \frac{1}{2}\langle \nabla_X V(X,t), X\Big(BB^\top \big(X^{-1}\nabla_X V(X,t)\big)^\vee\Big)^\wedge\rangle_X.\end{aligned} \tag{30}$$

Recall assumption 1, then the first order derivative of the minimum Hamiltonian (30) in a given tangent direction $X\Gamma$ yields

$$\begin{aligned}&\mathcal{D}_X\mathcal{H}^*(X,\nabla_X V(X,t),t)\circ X\Gamma = \\ &-\mathcal{D}_X^2 V(X,t)\circ\Big(X\Big(BB^\top\big(X^{-1}\nabla_X V(X,t)\big)^\vee\Big)^\wedge, X\Gamma\Big) \\ &-\mathcal{D}_X^2 V(X,t)\circ(XU, X\Gamma) - \mathcal{D}_X V(X,t)\circ X\,\mathbf{\Lambda}^x_\Gamma(U).\end{aligned} \tag{31}$$

Here, the connection $\mathbf{\Lambda}^x_\Gamma(U)$ for $x\in\{0,C\}$, was defined in (8) and (9).

Theorem 1: Let Assumption 1 hold. Then the following equation recursively computes the minimum-energy estimate $\hat{X}(t)$ and solves Problem 1.

$$\dot{\hat{X}}(t) = \hat{X}(t)U(t),\ \hat{X}(0) = \hat{X}_0. \tag{32}$$

Proof: Recall the definition for $\hat{X}(t)$ as given in (23). This can be equivalently expressed as $\nabla_X V(\hat{X}(t),t) = 0$ and therefore for any tangent direction $X\Gamma\in T_X\,\mathrm{SE}(3)$ it follows that

$$\{\mathcal{D}_X V(X,t)\circ X\Gamma = \langle \nabla_X V(X,t), X\Gamma\rangle_X\}_{X=\hat{X}(t)} = 0. \tag{33}$$

Following Mortensen's approach [19], one concludes that the total time derivative of the gradient $\nabla_X V(\hat{X}(t),t)$ is equal to zero too. Using the chain rule and the HJB equation (29) we obtain

$$\begin{aligned}&\{\langle\frac{d}{dt}(\nabla_X V(X,t)), X\Gamma\rangle_X\}_{X=\hat{X}(t)} = 0, \\ \Rightarrow&\{\mathcal{D}_X^2 V(X,t)\circ(X\Gamma,\dot{\hat{X}}(t)) + \\ &\mathcal{D}_X\frac{\partial}{\partial t}V(X,t)\circ X\Gamma\}_{X=\hat{X}(t)} = 0, \\ \Rightarrow&\{\mathcal{D}_X^2 V(X,t)\circ(X\Gamma,\dot{\hat{X}}(t)) + \\ &\mathcal{D}_X\mathcal{H}^*(X,\nabla_X V(X,t),t)\circ X\Gamma\}_{X=\hat{X}(t)} = 0.\end{aligned} \tag{34}$$

Next, replace the equality (31) into above, note that the first and the last terms in (31) when evaluated at $X=\hat{X}(t)$ yield zero due to (33), and note that Definition 1 is used. Equation (32) follows. The initial condition $\hat{X}(0)$ is derived directly from the initial condition for the value function in (22). ∎

Even though we are predominantly concerned with a recursive minimum-energy estimate $\hat{X}(t)$ it is often useful to also recursively calculate matrix $P(t)$, introduced in Definition 1, as it encodes the covariance or a measure of uncertainty of the estimate $\hat{X}(t)$.

Theorem 2: Let assumptions 1 and 2 hold. Then the Hessian of the value function (Definition 1) is recursively obtained from the following two equations depending on the choice of $\mathrm{SE}(3)$ connection defined in (7). Let $P^0(0)=P_0$, the zero connection (8) yields

$$\dot{P}^0(t) = -P^0BB^\top P^0 + 2\mathbb{P}_s(P^0\begin{bmatrix}0.5(U_\omega)_\times & 0_{3\times3}\\ (U_v)_\times & 0_{3\times3}\end{bmatrix}). \tag{35}$$

Alternatively, let $P^C(0)=P_0$, the Cartan connection (9) yields

$$\dot{P}^C(t) = -P^CBB^\top P^C + \mathbb{P}_s(P^C\begin{bmatrix}(U_\omega)_\times & 0_{3\times3}\\ (U_v)_\times & (U_\omega)_\times\end{bmatrix}). \tag{36}$$

Proof: The time evolution of the Hessian can be calculated by performing a total time derivative of (26) and taking into account either of the zero or Cartan connections. For $x\in\{0,C\}$ and any two tangent directions $X\Gamma, X\Psi\in T_X\,\mathrm{SE}(3)$ we obtain

$$\begin{aligned}&\langle\dot{P}^x\Gamma^\vee,\Psi^\vee\rangle = \langle\frac{d}{dt}(\mathbf{Hess}_X\,V(X,t))\circ X\Gamma, X\Psi\rangle_{X=\hat{X}(t)} = \\ &\{\mathcal{D}_X^2\mathcal{H}^*(X,\nabla_X V(X,t),t)\circ(X\Gamma,X\Psi)\}_{X=\hat{X}(t)} = \\ &\{-\mathcal{D}_X^2 V(X,t)\circ\Big(\mathbf{Hess}_X\,V(X,t)\circ X\big(BB^\top\Gamma^\vee\big)^\wedge, X\Psi\Big) \\ &-\mathcal{D}_X^2 V(X,t)\circ(X\,\mathbf{\Lambda}^x_\Psi(U), X\Gamma) \\ &-\mathcal{D}_X^2 V(X,t)\circ(X\,\mathbf{\Lambda}^x_\Gamma(U), X\Psi)\}_{X=\hat{X}(t)}.\end{aligned} \tag{37}$$

Note that we used the HJB (29), and the fact that the value function is assumed to be quadratic to obtain the second step of the above. The final step of the above is done by replacing (31). The rest of the proof follows by replacing the connection with either the zero or the Cartan connection and by utilizing (33). ∎

Now let us consider Problem 2.

Theorem 3: Consider the landmark measurement $\bar{y}(t)$ obtained according to (19). Assume that the updated value function $V^+(X,t)$ is quadratic in X when evaluated at $X=\hat{X}^+(t)$. Then the following equations solve problem 2 and yield two sets of discrete update equations for $\hat{X}^+(t)$ and the matrices $P^{0+}(t)$ and $P^{C+}(t)$, representing the updated Hessian $\mathbf{Hess}_X\,V^+(X,t)$ evaluated at $\hat{X}^+(t)$ and calculated using the zero connection (8) and the Cartan connection (9), respectively.

The zero connection (8) yields the discrete update equations

$$\begin{aligned}&\hat{X}^{0+}(t) \coloneqq \hat{X}^+(\hat{X}(t),P^0(t),t), P_{\bar{y}} \coloneqq \tilde{D}\tilde{D}^\top,\ \hat{\bar{y}} \coloneqq \hat{X}^{-1}\bar{l}, \\ &\hat{X}^{0+}(t) = \hat{X}\exp\Big(\Big(-(P^{0+})^{-1}\mathbb{P}\big(P_{\bar{y}}^{-1}(\bar{y}-\hat{\bar{y}})\hat{\bar{y}}^\top\mathbf{2}\big)^\vee\Big)^\wedge\Big), \\ &P^{0+} = P^0 + Q^0,\ Q^0 \coloneqq \begin{bmatrix}Q^0_{11} & Q^0_{12}\\ (Q^0_{12})^\top & Q^0_{22}\end{bmatrix},\ P_y \coloneqq DD^\top, \\ &Q^0_{11} \coloneqq \hat{y}_\times^\top P_y^{-1}\hat{y}_\times + \mathbb{P}_t\big(\mathbb{P}_s(P_y^{-1}(y-\hat{y})\hat{y}^\top)\big), \\ &Q^0_{12} \coloneqq (P_y^{-1}(y-\hat{y}))_\times + \hat{y}_\times P_y^{-1},\ Q^0_{22} \coloneqq P_y^{-1}.\end{aligned} \tag{38}$$

The Cartan connection (9) on the other hand yields the

following alternative discrete update equations.

$$\hat{X}^{C+}(t) \coloneqq \hat{X}^{+}(\hat{X}(t), P^{C}(t), t), P_{\bar{y}} \coloneqq \tilde{D}\tilde{D}^{\top},\ \hat{\bar{y}} \coloneqq \hat{X}^{-1}\bar{l},$$
$$\hat{X}^{C+}(t) = \hat{X}\exp\left(\left(-(P^{C+})^{-1}\mathbb{P}\big(P_{\bar{y}}^{-1}(\bar{y}-\hat{\bar{y}})\hat{\bar{y}}^{\top}\mathbf{2}\big)^{\vee}\right)^{\wedge}\right),$$
$$P^{C+} = P^{0} + Q^{C},\ Q^{C} \coloneqq \begin{bmatrix} Q_{11}^{C} & Q_{12}^{C} \\ (Q_{12}^{C})^{\top} & Q_{22}^{C}\end{bmatrix},\ P_{y} \coloneqq DD^{\top},$$
$$Q_{11}^{C} \coloneqq \hat{y}_{\times}^{\top}P_{y}^{-1}\hat{y}_{\times} + \mathbb{P}_{t}\big(\mathbb{P}_{s}(P_{y}^{-1}(y-\hat{y})\hat{y}^{\top})\big),$$
$$Q_{12}^{C} \coloneqq \frac{1}{2}(P_{y}^{-1}(y-\hat{y}))_{\times} + \hat{y}_{\times}P_{y}^{-1},\ Q_{22}^{C} \coloneqq P_{y}^{-1}. \tag{39}$$

Proof: Let us consider a Taylor series expansion of $V^{+}(X,t)$ around the nominal point $X = \hat{X}(t)$. Recall our assumption that $V^{+}(X,t)$ is quadratic.

$$V^{+}(X,t) = V^{+}(\hat{X}(t),t) + \langle \nabla_{X}V^{+}(\hat{X}(t),t), \hat{X}\log(\hat{X}^{-1}X)\rangle + \frac{1}{2}\langle \mathbf{Hess}_{X}\, V^{+}(\hat{X}(t),t)\circ \hat{X}\log(\hat{X}^{-1}X), \hat{X}\log(\hat{X}^{-1}X)\rangle. \tag{40}$$

From definition (25) and for any tangent direction $X\Gamma$ one has

$$\{\mathcal{D}_{X}V^{+}(X,t)\circ X\Gamma\}_{X=\hat{X}^{+}(t)} = 0. \tag{41}$$

Replace $V^{+}(X,t)$ from the RHS of (40).

$$0 = \{\langle \nabla_{X}V^{+}(\hat{X}(t),t), \hat{X}\tilde{\Gamma}\rangle + \langle \mathbf{Hess}_{X}\, V^{+}(\hat{X}(t),t)\circ \hat{X}\tilde{\Gamma}, \hat{X}\log(\hat{X}^{-1}X)\rangle\}_{X=\hat{X}^{+}(t)}. \tag{42}$$

Here $\hat{X}\tilde{\Gamma} \coloneqq \mathcal{D}_{X}(\hat{X}\log(\hat{X}^{-1}X))\circ X\Gamma)$ is a tangent direction which can be dropped from the two sides of the equation. The gradient and the Hessian in (42) can be calculated based on (24) and recalling that $\nabla_{X}V(\hat{X}(t),t) = 0$.

$$\nabla_{X}V^{+}(\hat{X}(t),t) = \hat{X}\mathbb{P}\big(P_{\bar{y}}^{-1}(\bar{y}-\hat{\bar{y}})\hat{\bar{y}}^{\top}\big),$$
$$\mathbf{Hess}_{X}\, V^{+}(\hat{X}(t),t) = \mathbf{Hess}_{X}\, V(\hat{X}(t),t) + \{\mathbf{Hess}_{X}(\frac{1}{2}\|\bar{y}(t) - X^{-1}(t)\bar{l}\|^{2}_{(\tilde{D}\tilde{D}^{\top})^{-1}})\}_{X=\hat{X}(t)}. \tag{43}$$

The two choices of connection (8) and (9) will result in different Hessian calculations resulting in the two update equations of the theorem. ∎

Note that Theorem 3 indicates how to optimally update the estimate and its covariance based on sporadically obtained landmark measurements. In previous work [23] it was shown that at least three non-collinear landmarks are required for well-posedness of the filtering problem and the favorable performance of filter.

V. Simulation Study

In this section, we provide a numerical example in order to demonstrate the performance of the proposed filters in Section IV.

Note that the implementation of the proposed equations is using the unit quaternion representation of rotations. The differential equations provided in (35) and (36) are numerically integrated by approximating the derivative from a first order Euler approximation. The time step of the simulation is $dt = 0.001$. The differential equations governing the quaternions however are implemented using the explicit solution of the exponential map that maintains their unit norm structure during integration. For more details we refer the reader to our previous works [17], [23]. The discrete landmark update steps are performed every $\Delta = 1000$ steps.

Consider the forward-left-up and the East-North-Up (ENU) standards for the x-y-z coordinates of the body fixed frame and the global reference frame, respectively [24]. Angular and translational velocities $\Omega = [0, 0, 1.5\sin(\frac{\pi}{9})]^{\top}$ and $V = [5, 0, 0]^{\top}$ drive a unicycle system trajectory and are measured in the body-fixed frame $\mathcal{B}$. These quantities are measured according to (18) with $B_{\omega} = 0.1I\,(\frac{rad}{s})$ and $B_{v} = 0.5I\,(\frac{m}{s})$. Note that we model $\delta_{\omega} = [0, 0, \delta_{z}]^{\top}, \delta_{v} = [\delta_{x}, 0, 0]$ where $\delta_{z}, \delta_{x} \sim \mathcal{N}(0,1)$ are random scalars drawn form the standard normal distribution $\mathcal{N}(0,1)$. Initial system coordinates is at $p(0) = [1, 2, 0]\,m$ and initial position estimates at $\hat{p}(0) = [3, -2, 0]\,m$. We also simulated 25° of initial rotation error for the filters. Both filters are starting with $P^{x}(0) = 10^{4}I,\ x \in \{0, C\}$. Two landmarks are considered located at $l_{1} = [-10, 15, 0]^{\top}\,m$ and $l_{2} = [0, 5, 0]^{\top}\,m$. Note that due to reduced degrees of freedom of the unicycle model, as compared to the full six degree of freedom pose dynamics, only two landmark measurements are sufficient for well-posedness of the filtering problem.

The landmark measurements are simulated based on (19) with $\epsilon = [\epsilon_{x}, \epsilon_{y}, 0]^{\top}\,m$, $\epsilon_{x}, \epsilon_{y} \sim \mathcal{N}(0,1)$. The error coefficient matrix is set at $D = 0.1I\,m$. Figure 1 shows the trajectories of the system and the two proposed filters in the x-y plane. Figure 2 compares the estimation error incurred in the attitude of the two filters, as measured by the angle of rotation. Figure 3 compares the estimation error incurred in the translation part of the filters, as Euclidean distance of estimated positions to the true positions. As can be seen, the two proposed filters yield reliable pose estimation despite the large measurement errors and the low frequency of discrete updates. Although there is no clear difference between the two filters in steady state, the one based on the symmetric Cartan connection initially outperforms the the zero connection based filter. This can be related to a difference observed in the two covariance forward propagation equations (35) and (36). Namely, in the latter, the linear term has a nonzero direct element for the covariance of position estimate while in the former this is zero.

VI. Conclusion

In this paper we extended our previous work on $\mathrm{SE}(3)$ and geometric filtering [17], [18] to allow for discrete time measurement updates. We showed how the two choices of affine connections on $\mathrm{SE}(3)$ result in two different filters. This was first pointed out in previous work [25] on minimum-energy filtering on general Lie groups but with no particularized derivation for $\mathrm{SE}(3)$. Our simulation study indicates that both filters work well in a difficult filtering scenario including large measurement errors and low frequency of discrete updates. Moreover, the proposed filter based on the Cartan

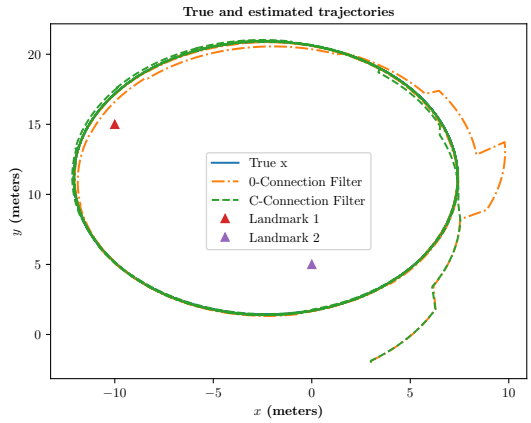

Fig. 1. Trajectories of the system the two proposed filters

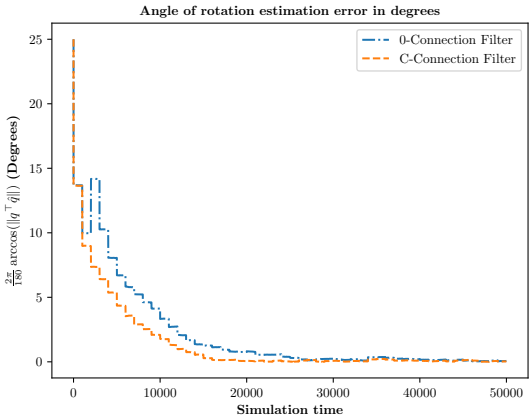

Fig. 2. Comparison in terms of angle of rotation estimation error

connection outperforms the proposed zero connection filter in the transient performance observed in the simulation.

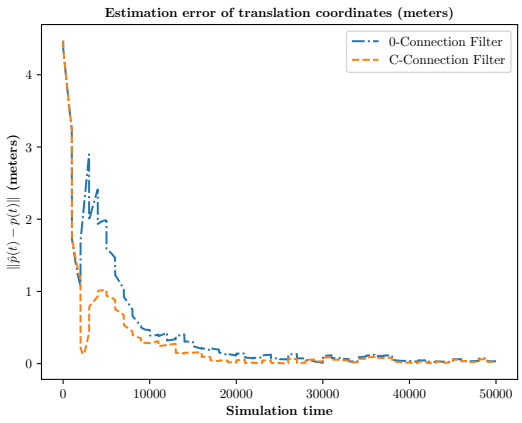

Fig. 3. Comparison in terms of position estimation error

REFERENCES

[1] F. Markley, "Multiplicative vs. additive filtering for spacecraft attitude determination," *Dynamics and Control of Systems and Structures in Space*, 2004.

[2] J. L. Crassidis, F. L. Markley, and Y. Cheng, "Survey of nonlinear attitude estimation methods," *Journal of Guidance Control and Dynamics*, vol. 30, pp. 12–28, 2007.

[3] B. D. O. Anderson and J. Moore, *Optimal filtering*. Prentice Hall, 1979.

[4] R. E. Kalman and R. S. Bucy, "New results in linear filtering and prediction theory," *Journal of Basic Engineering*, vol. 83, no. 3, pp. 95–108, 1961.

[5] S. Salcudean, "A globally convergent angular velocity observer for rigid body motion," *IEEE Transactions on Automatic Control*, vol. 36, no. 12, pp. 1493–1497, 1991.

[6] R. Mahony, T. Hamel, and J. -M. Pflimlin, "Nonlinear complementary filters on the special orthogonal group," *IEEE Transactions on Automatic Control*, vol. 53, no. 5, pp. 1203–1218, 2008.

[7] G. Baldwin, R. Mahony, and J. Trumpf, "A nonlinear observer for 6 DOF pose estimation from inertial and bearing measurements," in *Robotics and Automation, 2009. ICRA'09. IEEE International Conference on*. IEEE, 2009, pp. 2237–2242.

[8] C. Lageman, J. Trumpf, and R. Mahony, "Gradient-like observers for invariant dynamics on a Lie group," *IEEE Transactions on Automatic Control*, vol. 55, no. 2, pp. 367–377, 2010.

[9] P. Martin and E. Salaun, "Invariant observers for attitude and heading estimation from low-cost inertial and magnetic sensors," in *Decision and Control, 2007 46th IEEE Conference on*, 2007, pp. 1039–1045.

[10] M.-D. Hua, T. Hamel, R. Mahony, and J. Trumpf, "Gradient-like observer design on the special euclidean group se (3) with system outputs on the real projective space," in *2015 54th IEEE Conference on Decision and Control (CDC)*. IEEE, 2015, pp. 2139–2145.

[11] D. E. Zlotnik and J. R. Forbes, "Higher-order nonlinear complementary filtering on lie groups," *IEEE Transactions on Automatic Control*, 2018.

[12] J. Reis, P. Batista, P. Oliveira, and C. Silvestre, "Nonlinear attitude observer on so (3) based on single body-vector measurements," in *2018 IEEE Conference on Control Technology and Applications (CCTA)*. IEEE, 2018, pp. 1319–1324.

[13] M. Wang and A. Tayebi, "Hybrid pose and velocity-bias estimation on $se(3)$ using inertial and landmark measurements," *IEEE Transactions on Automatic Control*, 2018.

[14] A. Barrau and S. Bonnabel, "Invariant kalman filtering," *Annual Review of Control, Robotics, and Autonomous Systems*, vol. 1, pp. 237–257, 2018.

[15] S. Bonnabel, "Left-invariant extended Kalman filter and attitude estimation," in *Proceedings of the IEEE Conference on Decision and Control*, 2007, pp. 1027–1032.

[16] P. Martin, E. Salaün, *et al.*, "Generalized multiplicative extended kalman filter for aided attitude and heading reference system," in *Proceedings of 2010 AIAA Guidance, Navigation, and Control Conference*, 2010.

[17] M. Zamani, J. Trumpf, and R. Mahony, "Minimum-energy filtering for attitude estimation," *IEEE Transactions on Automatic Control*, vol. 58, no. 11, pp. 2917–2921, 2013.

[18] ——, "Minimum-energy pose filtering on the special Euclidean group," in *Proceedings of the 20th International Symposium on Mathematical Theory of Networks and Systems (MTNS), 2012. Paper no. 189.*

[19] R. E. Mortensen, "Maximum-likelihood recursive nonlinear filtering," *Journal of Optimization Theory and Applications*, vol. 2, no. 6, pp. 386–394, 1968.

[20] O. B. Hijab, "Minimum energy estimation," Ph.D. dissertation, University of California, Berkeley, 1980.

[21] M. Izadi, A. K. Sanyal, and R. R. Warier, "Variational attitude and pose estimation using the lagrange-dalembert principle," in *2018 IEEE Conference on Decision and Control (CDC)*. IEEE, 2018, pp. 1270–1275.

[22] M. Zamani, J. Trumpf, and R. Mahony, "Nonlinear attitude filtering: A comparison study," *arXiv preprint arXiv:1502.03990*, 2015.

[23] M.-D. Hua, M. Zamani, J. Trumpf, R. Mahony, and T. Hamel, "Observer design on the special Euclidean group SE(3)," in *Proceedings of the 50th IEEE Conference on Decision and Control*, 2011, pp. 8169–8175.

[24] "Ros rep-103," Available online:, access March 2018. [Online]. Available: http://www.ros.org/reps/rep-0103.html

[25] A. Saccon, J. Trumpf, R. Mahony, and A. P. Aguiar, "Second-order-optimal filters on lie groups," in *52nd IEEE Conference on Decision and Control*. IEEE, 2013, pp. 4434–4441.